Available online at http://ijcpe.uobaghdad.edu.iq and www.iasj.net
Iraqi Journal of Chemical and Petroleum Engineering
Vol. 24 No.1 (March 2023) 27 – 31
EISSN: 2618-0707, PISSN: 1997-4884

Measurement and Analysis of Bubble Size Distribution in the Electrochemical Stirred Tank Reactor

Raghad S. Mahmood [a], Alanood A. Alsarayreh [b], and Ammar S. Abbas [a, *]

[a] *Chemical Engineering Department, College of Engineering, University of Baghdad, Iraq*
[b] *Chemical Engineering Department, Faculty of Engineering, Mutah University, P.O. Box 7, Karak 61710, Jordan*

Abstract

The dimensions of bubbles were measured in a stirrer tank electrochemical reactor, where the analysis of the bubble size distribution has a substantial impact on the flow dynamics. The high-speed camera and image processing methods were used to obtain a reliable photo. The influence of varied air flow rates (0.3; 0.5; 1 l/min) on BSD was thoroughly investigated. Two types of distributors (cubic and circular) were examined, and the impact of various airflow rates on BSD was investigated in detail. The results showed that the bubbles for the two distributors were between 0.5 and 4.5 mm. For both distributors at each airflow, the Sauter mean diameter for the bubbles was calculated. According to the results, as the flow rate raised, the bubble size for cubic distributors increased from 2.35 to 2.41 mm and for circular distributors from 2.76 to 2.88 mm.

Keywords: Electrochemical, Bubble size distribution, reactor, mean diameter.

Received on 01/07/2022, Received in Revised Form on 26/08/2022, Accepted on 27/08/2022, Published on 30/03/2023

https://doi.org/10.31699/IJCPE.2023.1.4

1- Introduction

Many industrial processes generate toxic and polluted wastewater that is difficult to degrade and requires costly physical or physic-chemical treatments [1]. One of the most essential and efficient treatment methods is electro-oxidation, which has become a viable alternative for wastewater treatment via redox reactions. As a result, the electrochemical reactor (ECR) systems have great interest daily [2, 3].

The continuous stirred tank electrochemical reactor with gas-liquid flow is commonly used in wastewater treatment plants as multiphase reactors. Bubble reactors are employed in several process industries because of their simple structure and ease of use [4]. The dispersed aeration is the dominant parameter that enhances oxygen transmission in several applications. The aeration involves the diffusion of air into the liquid in the form of bubbles through small holes of a distributor [5]. The performance of gas-liquid systems is affected by the dispersion of the gas into the reactor. Tiny bubbles with a uniform distribution over the equipment's cross section are preferred to increase the interfacial area and enhance transport phenomena [6].

One of the most critical parameters impacting the efficiency of this form of operation is the contact time of air bubbles with the liquid. The contact time depends on the size of the bubble, its terminal velocity, diffuser submergence, and water velocity [7]. The speed of a bubble in a continuous fluid is affected by many physical properties, such as the density, viscosity, and surface tension of both gas and liquid, as well as by outside factors, such as mixing conditions [8].

The bubble size distribution (BSD) is a significant parameter in reactor design and the performance of gas-liquid contact [9]. Large bubbles prefer to escape quickly at the top surface, whereas tiny bubbles are more likely to reach the side wall and mold depth. Also, tiny bubbles increase the gas-liquid interface area, the contact time between the air bubble and the water rises, and the mass transfer process and flow behavior change [10,11]. For optimizing bubble reactor processes, knowing the BSD in the specific system under various operating conditions is crucial. However, the BSD in an industrial bubble reactor is extremely challenging to quantify. In order to analyse the bubble size, various types of laboratory-scale bubble reactors have been used [12]. Intrusive and non-intrusive techniques can be used to measure BSD. Non-intrusive techniques, such as image analysis of bubble photos, are often favored since they do not impact the reactor's hydrodynamics [13-15]. The high-speed camera captures the bubble images directly, retrieving image features through digital image processing to determine bubble sizes and their distribution [16,17].

The goal of this work is to figure out the bubble size distribution for two types of distributors in a continuous stirred tank electrochemical reactor and figure out the Sauter mean diameter for each distributor at different air flow rates.

*Corresponding Author: Name: Ammar S. Abbas, Email: ammarabbas@coeng.uobaghdad.edu.iq

2- Experimental Work

Using a camera (Nikon D750, 1/20000s), 24 megapixels, and an objective lens (Nikon 40X), connected to a high-speed flash source (NiceFoto n4). The camera was also connected to the PC (Laptop type Lenovo Legion y530) to analyze the images by computer programming. All parts of the camera were self-assembled and designed. The dimensions of the bubbles were photographed in a glass box with dimensions of (15 cm × 22 cm × 17cm) in length, width, and height, respectively. Air bubbles were introduced through the distributor in the test region of the box at the required flow rate. The camera and the flash were operated. Images were taken of the bubbles while they were rising throughout the water. These images appeared on the laptop screen and were recorded. Images were captured near the box wall nearest the camera, pointing at the reactor's centerline to reduce image distortion. In this situation, the bubbles along the wall are assumed to be typical of those within the box. Two types of distributors were tested, cubic (sands and stone; 12 x 25 mm) and circular (sands and stone, plastic; 10.1 x 6.9 x 1.2 cm; hole diameter: 3 mm). Each air distributor was photographed at (0.3, 0.5, 1 l/min) air flow rates. Several images were captured while the bubbles were rising in the liquid, and then the photos were processed by ImageJ software [18] to calculate the size of the bubbles. A reference scale was used for calibration, and after that, an 'analysis tool' was used to measure the effective bubble diameter. Fig. 1 shows the schematic diagram of the lab-scale system.

The bubble size distribution was characterized by Sauter mean diameter (d_s). Its expression is given by Eq. 1 [19]:

$$d_s = \frac{\sum n_i d_i^3}{\sum n_i d_i^2} \quad (1)$$

Where d_i is the bubble diameter (mm) and n_i is the number of bubbles of diameter d_i. The relative frequency can be determined as the ratio between the number of bubbles in each range and the total number of bubbles.

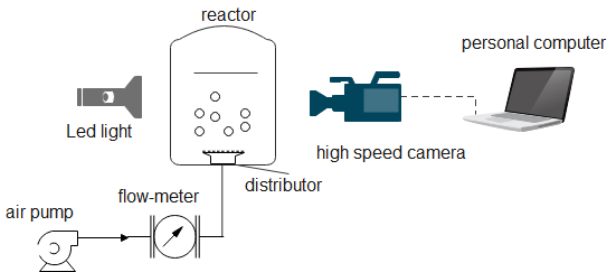

Fig. 1. Schematic Diagram of the Lab-Scale System

3- Results and Discussion

The photographic method was used to determine the size of the bubbles at different air flow rates (0.3; 0.5; 1 l/min).

Fig. 2, and Fig. 3 show the photographed bubbles at 0.3; 0.5; 1 l/min for cubic and circular distributors, respectively. The only clear images in all the photographs are of bubbles near the vessel wall. Some bubbles do not have a perfect sphere shape, but an oblate spheroid can be used to approximate it. It can also be observed that the bubble size is not uniform in all images. The ImageJ program processed the photos, and the Sauter mean diameter of the bubble for each distributor was calculated.

Fig. 4 shows the cubic distributor's BSD. It can be observed from Figure 4 at a flow rate of 0.3 l/min that bubbles with diameters ranging from 2 to 2.5 mm have a greater relative frequency when compared to other ranges. Furthermore, with approximately 40%, the 2-2.5 mm range was the most dominating. At an airflow rate of 0.5 l/min, bubbles with diameters ranging from 1.5 to 2 mm have a higher relative frequency of 0.37. As a result, the size range between 1.5-2 mm was the most dominating range. Figure 4 presents BSD at a flow rate of 1 l/min. Bubbles with sizes between 1 and 1.5 mm have a relative frequency of 0.37. The lowest relative frequency was observed between the bubble diameters of 0.5-1, 3-3.5, and 3.5-4 mm.

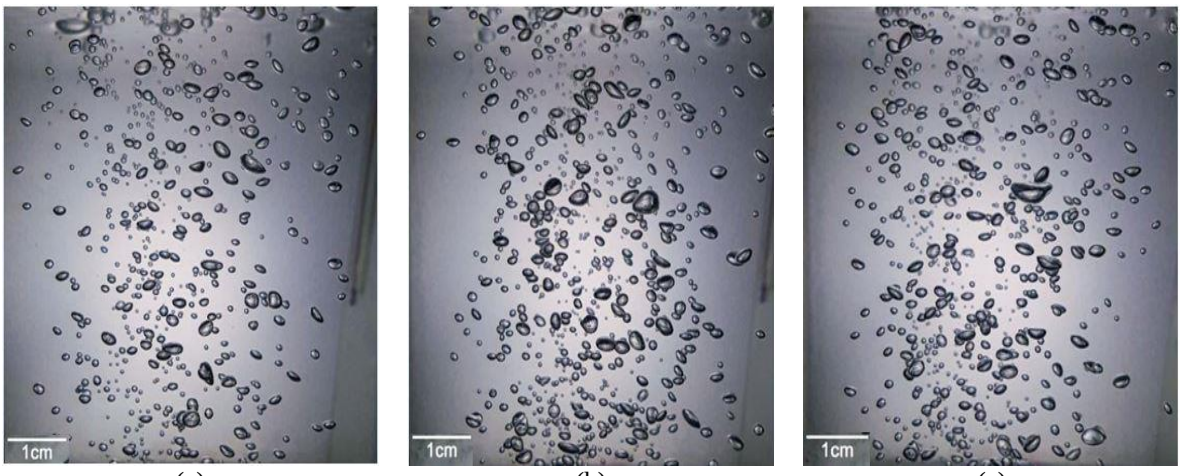

(a) (b) (c)

Fig. 2. Cubic Distributor Bubbles (a: 0.3l/min; b: 0.5 l/min; c: 1 l/min)

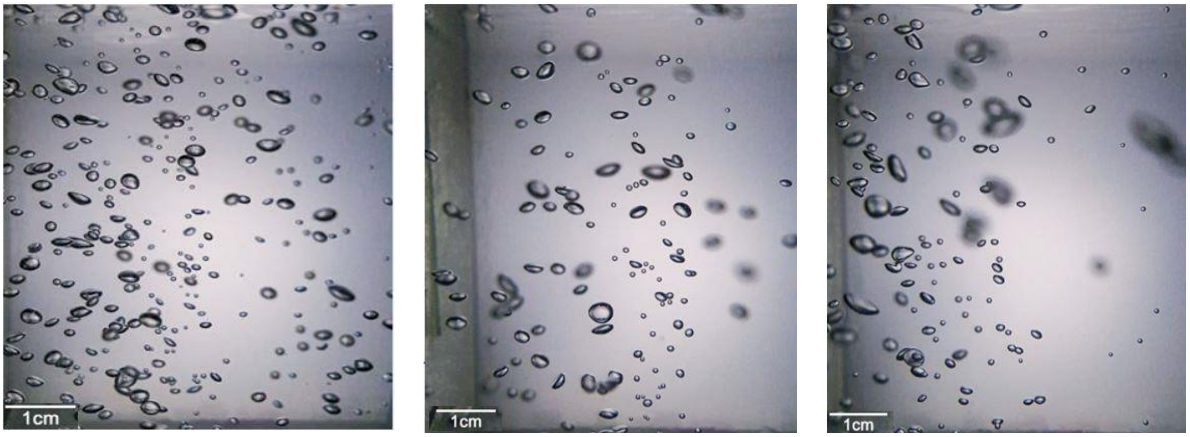

(a) (b) (c)

Fig. 3. Circular Distributor Bubbles (a: 0.3 l/min; b: 0.5 l/min; c: l/min)

Fig. 5 shows BSD for a circular distributor at 0.3, 0.5, and 1 l/min. At air flow rate of 0.3 l/min, Fig. 4 indicates that the higher relative frequency was at bubble size from 1.5 to 2 mm range which reached 0.47; thus, the size range between 1.5-2 was the most dominating range. At 0.5 l/min, the same dominant range was observed with a relative frequency of 0.3. In comparison, the lowest relative frequency was in the size range between 4-4.5 mm. Figure 4 noted that at 1 l/min, the lowest relative frequency was observed between the bubble diameters of 3.5-4 mm. The most dominant range (approximately 35%) was clearly between 0.5-1 mm.

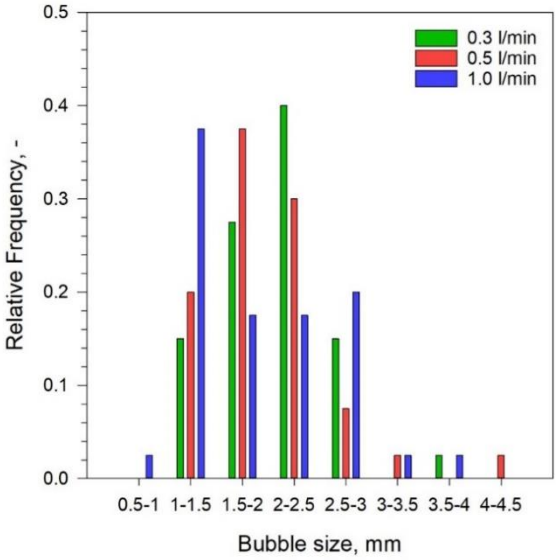

Fig. 4. BSD for Cubic Distributor (0.3 l/min; 0.5 l/min; 1 l/min)

Table 1 represents the Sauter mean diameter (d_s) value for the bubbles of cubic and circular distributors calculated from Eq. 1. At 0.3 l/min, the cubic distributor bubbles' size was equal to 2.35 mm, which is smaller than the size of the bubbles for the circular distributor (2.76 mm). As the airflow increases, the bubble size of both distributors increases from 2.35 mm to 2.41 mm for the cubic distributor and from 2.76 mm to 3.88 mm for the circular distributor, but the bubble size of the cubic distributor remains smaller than the bubble size of the circular distributor. This increase in the size of the bubbles occurred because the airflow rate directly contributes to the bubble expansion process during bubble formation. The higher the flow rate, the faster the bubble forms, resulting in a larger bubble size. Since it is known that the smallest bubble size is the best air distributor thus, the cubic distributor has been selected.

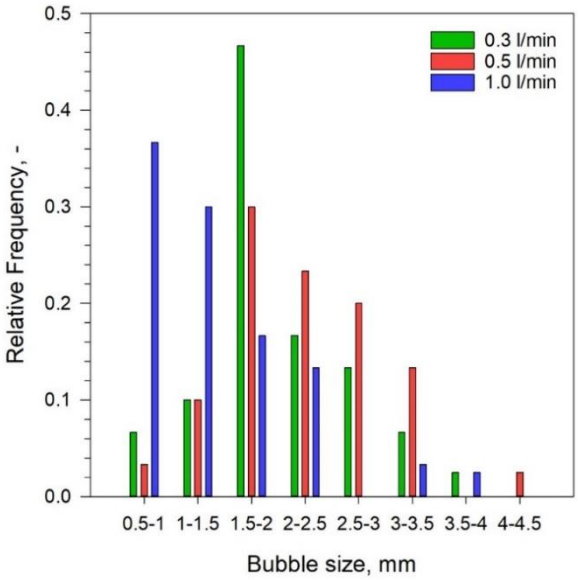

Fig. 5. BSD for Circular Distributor (0.3 l/min; 0.5 l/min; 1l/min)

Table 1. The Value of Sauter Mean Diameter for the Bubbles of Cubic and Circular Distributor

Air flow rate (l/min)	d_s (mm)	
	Cubic distributor	Circular distributor
0.3	2.35	2.76
0.5	2.38	2.98
1	2.41	3.88

4- Conclusion

BSD and the Sauter mean diameter for the two-phase continuous stirred tank electrochemical reactor were

measured photographically. Two types of distributors were studied at different air flow rates (0.3; 0.5; 1 l/min). The results show that the highest relative frequency for a cubic distributor at 0.3 l/min was at bubble diameters ranging between 2 to 2.5 mm. In comparison, at 0.5 l/min the bubbles with diameters ranging from 1.5 to 2 mm have a higher relative frequency. The bubble size range between 1-1.5 mm has a higher relative frequency at 1 l/min. For circular distributor, the highest relative frequency ranged between 1.5-2 mm at 0.3 l/min and 0.5 l/min, 0.5-1 mm at 1 l/min. The Sauter mean diameter of the bubbles was increased with an increase in the airflow rate for each distributor. Still, the cubic distributor has a smaller bubble size than the circular distributor under all conditions.

References

[1] B. K. Körbahti and A. Tanyolaç, "Modeling of a continuous electrochemical tubular reactor for phenol removal," *Chem. Eng. Commun.*, vol. 190, no. 5–8, pp. 749–762, 2003, https://doi.org/10.1080/00986440302129.

[2] F. C. Walsh, "Electrochemical technology for environmental treatment and clean energy conversion," *Pure Appl. Chem.*, vol. 73, no. 12, pp. 1819–1837, 2001, https://doi.org/10.1351/pac200173121819.

[3] R. S. Mahmood and A. S. Abbas, "Validation of a Three-parameters Hydrodynamic Model to Describe the non-ideal Flow in a Continuous Stirred Tank Reactor of the Electro-Fenton Oxidation of Organic Pollutants in Wastewater," *J. Phys. Conf. Ser.*, vol. 1973, no. 1, p. 012092, 2021, http://doi.org/10.1088/1742-6596/1973/1/012092.

[4] H. Wang, X. Jia, X. Wang, Z. Zhou, J. Wen, and J. Zhang, "CFD modeling of hydrodynamic characteristics of a gas-liquid two-phase stirred tank," *Appl. Math. Model.*, vol. 38, no. 1, pp. 63–92, 2014, https://doi.org/10.1016/j.apm.2013.05.032.

[5] W. H. Zhang, X. Jiang, and Y. M. Liu, "A method for recognizing overlapping elliptical bubbles in bubble image," *Pattern Recognit. Lett.*, vol. 33, no. 12, pp. 1543–1548, 2012, https://doi.org/10.1016/j.patrec.2012.03.027.

[6] M. Polli, M. Di Stanislao, R. Bagatin, E. A. Bakr, and M. Masi, "Bubble size distribution in the sparger region of bubble columns," *Chem. Eng. Sci.*, vol. 57, no. 1, pp. 197–205, 2002, https://doi.org/10.1016/S0009-2509(01)00301-3.

[7] D. S. Mavinic and J. K. Bewtra, "Bubble size and contact time in diffused aeration systems," *J. Water Pollut. Control Fed.*, vol. 46, no. 9, pp. 2129–2137, 1974.

[8] M. S. N. Oliveira, A. W. Fitch, and X. Ni, "A Study of Bubble Velocity and Bubble Residence Time in a Gassed Oscillatory Baffled Column Effect of Oscillation Frequency," *Engineering*, vol. 81, no. February, 2003, https://doi.org/10.1205/026387603762878692.

[9] S. Capela, M. Roustan, and A. Héduit, "Transfer number in fine bubble diffused aeration systems," *Water Sci. Technol.*, vol. 43, no. 11, pp. 145–152, 2001, https://doi.org/10.2166/wst.2001.0677.

[10] W. Yang, Z. Luo, N. Zhao, and Z. Zou, "Numerical Analysis of Effect of Initial Bubble Size on Captured Bubble Distribution in Steel Continuous Casting Using Euler-Lagrange Approach Considering Bubble Coalescence and Breakup Weidong," 2020, https://doi.org/10.3390/met10091160.

[11] H. J. B. Couto, D. G. Nunes, R. Neumann, and S. C. A. França, "Micro-bubble size distribution measurements by laser diffraction technique," *Miner. Eng.*, vol. 22, no. 4, pp. 330–335, 2009, https://doi.org/10.1016/j.mineng.2008.09.006.

[12] Y. M. Lau, K. T. Sujatha, M. Gaeini, N. G. Deen, and J. A. M. Kuipers, "Experimental study of the bubble size distribution in a pseudo-2D bubble column," *Chem. Eng. Sci.*, vol. 98, pp. 203–211, 2013, https://doi.org/10.1016/j.ces.2013.05.024.

[13] D. Mesa and P. R. Brito-Parada, "Bubble size distribution in aerated stirred tanks: Quantifying the effect of impeller-stator design," *Chem. Eng. Res. Des.*, vol. 160, no. 1, pp. 356–369, 2020, https://doi.org/10.1016/j.cherd.2020.05.029.

[14] G. G. Bellido, M. G. Scanlon, J. H. Page, and B. Hallgrimsson, "The bubble size distribution in wheat flour dough," *Food Res. Int.*, vol. 39, no. 10, pp. 1058–1066, 2006, https://doi.org/10.1016/j.foodres.2006.07.020.

[15] T. Wang, Z. Xia, and C. Chen, "Computational study of bubble coalescence/break-up behaviors and bubble size distribution in a 3-D pressurized bubbling gas-solid fluidized bed of Geldart A particles," *Chinese J. Chem. Eng.*, vol. 44, pp. 485–496, 2022, https://doi.org/10.1016/j.cjche.2021.03.040.

[16] T. Xue, X. W. Liu, Y. X. Jin, and B. Wu, "Bubbles image processing and parameters measurement based on the high-speed photography," *Seventh Int. Symp. Precis. Eng. Meas. Instrum.*, vol. 8321, p. 83210T, 2011, https://doi.org/10.1117/12.903860.

[17] R. S. Mahmood, A. S. Abbas, and International Scientific Conference Marshes Research Center, "Internals Design of Continuous Stirred Tank Electrochemical Reactor Based on the Residence Time Distribution Approach," *Egypt. J. Chem.*, 2022, http://doi.org/10.21608/EJCHEM.2022.122976.5502.

[18] C. A. Schneider, W. S. Rasband, and K. W. Eliceiri, "NIH Image to ImageJ: 25 years of image analysis," *Nat. Methods*, vol. 9, no. 7, pp. 671–675, 2012, http://doi.org/10.1038/nmeth.2089.

[19] M. Senouci-Bereksi, F. K. Kies, and F. Bentahar, "Hydrodynamics and Bubble Size Distribution in a Stirred Reactor," *Arab. J. Sci. Eng.*, vol. 43, no. 11, pp. 5905–5917, 2018, https://doi.org/10.1080/00986440302129.

قياس و تحليل توزيع حجم الفقاعات في مفاعل الخزان الكهروكيميائي

رغد ساجد محمود [١]، العنود الصرايرة [٢]، وعمار صالح عباس [١،*]

١ قسم الهندسة الكيمياوية، كلية الهندسة، جامعة بغداد، بغداد، العراق
٢ قسم الهندسة الكيمياوية، جامعة موته، الاردن

الخلاصة

يتم قياس أبعاد الفقاعات في مفاعل كهروكيميائ مستمر، حيث يكون لتحليل توزيع حجم الفقاعة تأثير كبير على ديناميكيات التدفق. تم استخدام كاميرا عالية السرعة و تقنيات معالجة الصور للحصول على صورة موثوقة. تم اختبار نوعين من الموزعات (مكعب و دائري)، و دُرست تأثير معدلات تدفق الهواء المختلفة (٠,٣، ١ لتر / دقيقة) على توزيع حجم الفقاعة بالتفصيل. تظهر النتائج أن حجم الفقاعات يتراوح بين ٠,٥ إلى ٤,٥ ملم للموزعين. تم حساب متوسط قطر الفقاعات لكلا الموزعين عند كل تدفق هواء. أشارت النتائج إلى زيادة حجم الفقاعة من ٢,٣٥ إلى ٢,٤١ مم للموزع المكعب ومن ٢,٧٦ إلى ٢,٨٨ مم للموزع الدائري عند زيادة معدل التدفق.

الكلمات الدالة: الكهروكيميائية، توزيع حجم الفقاعات، المفاعل، متوسط القطر.